

## Electronic Supplementary Information (ESI)

for

### A new spinel high-entropy oxide ( $\text{Mg}_{0.2}\text{Ti}_{0.2}\text{Zn}_{0.2}\text{Cu}_{0.2}\text{Fe}_{0.2}$ )<sub>3</sub>O<sub>4</sub> with fast reaction kinetic and excellent stability as anode materials for lithium ion batteries

Hong Chen,<sup>a</sup> Nan Qiu,<sup>a,\*</sup> Baozhen Wu,<sup>a</sup> Zhaoming Yang,<sup>a</sup> Sen Sun,<sup>a</sup> and Yuan Wang<sup>a,\*</sup>

<sup>a</sup> Key Laboratory of Radiation Physics and Technology, Ministry of Education, Institute of Nuclear Science and Technology, Sichuan University, Chengdu 610064, People's Republic of China.

\* Corresponding authors

E-mail: qiun@scu.edu.cn (N. Q.) and wyuan@scu.edu.cn (Y. W.)

#### Table of Contents:

<b>Figure S1.</b> EDS analysis result of the synthesized ( $\text{Mg}_{0.2}\text{Ti}_{0.2}\text{Zn}_{0.2}\text{Cu}_{0.2}\text{Fe}_{0.2}$ ) <sub>3</sub> O <sub>4</sub> particles.
<b>Figure S2.</b> N <sub>2</sub> adsorption-desorption isotherms and the BJH pore size distribution curves of the synthesized ( $\text{Mg}_{0.2}\text{Ti}_{0.2}\text{Zn}_{0.2}\text{Cu}_{0.2}\text{Fe}_{0.2}$ ) <sub>3</sub> O <sub>4</sub> particles.
<b>Figure S3.</b> XPS survey scan spectrum of the synthesized ( $\text{Mg}_{0.2}\text{Ti}_{0.2}\text{Zn}_{0.2}\text{Cu}_{0.2}\text{Fe}_{0.2}$ ) <sub>3</sub> O <sub>4</sub> particles.
<b>Figure S4.</b> High-resolution XPS spectra of the synthesized ( $\text{Mg}_{0.2}\text{Ti}_{0.2}\text{Zn}_{0.2}\text{Cu}_{0.2}\text{Fe}_{0.2}$ ) <sub>3</sub> O <sub>4</sub> particles.
<b>Figure S5.</b> SEM results of the evolution process of ( $\text{Mg}_{0.2}\text{Ti}_{0.2}\text{Zn}_{0.2}\text{Cu}_{0.2}\text{Fe}_{0.2}$ ) <sub>3</sub> O <sub>4</sub> electrodes at a current density of 100 mA g <sup>-1</sup> .
<b>Figure S6.</b> Correlation between the scan rates and corresponding currents of the ( $\text{Mg}_{0.2}\text{Ti}_{0.2}\text{Zn}_{0.2}\text{Cu}_{0.2}\text{Fe}_{0.2}$ ) <sub>3</sub> O <sub>4</sub> electrode
<b>Figure S7.</b> The capacitive contribution to the total current contribution for the ( $\text{Mg}_{0.2}\text{Ti}_{0.2}\text{Zn}_{0.2}\text{Cu}_{0.2}\text{Fe}_{0.2}$ ) <sub>3</sub> O <sub>4</sub> electrode at 0.1-0.8 mV s <sup>-1</sup> vs. Li <sup>+</sup> /Li.
<b>Table S1.</b> The comparison of lattice parameter, BET surface area values between ( $\text{Mg}_{0.2}\text{Ti}_{0.2}\text{Zn}_{0.2}\text{Cu}_{0.2}\text{Fe}_{0.2}$ ) <sub>3</sub> O <sub>4</sub> and some other solid solutions reported in literature.
<b>Table S2.</b> Summary of electrochemical performance of different transition metal oxides as anode materials for lithium ion batteries.
<b>Table S3.</b> The kinetic parameters of the fresh ( $\text{Mg}_{0.2}\text{Ti}_{0.2}\text{Zn}_{0.2}\text{Cu}_{0.2}\text{Fe}_{0.2}$ ) <sub>3</sub> O <sub>4</sub> half-cell and the half-cell charged to 3.0 V after 300 discharge/charge cycles.

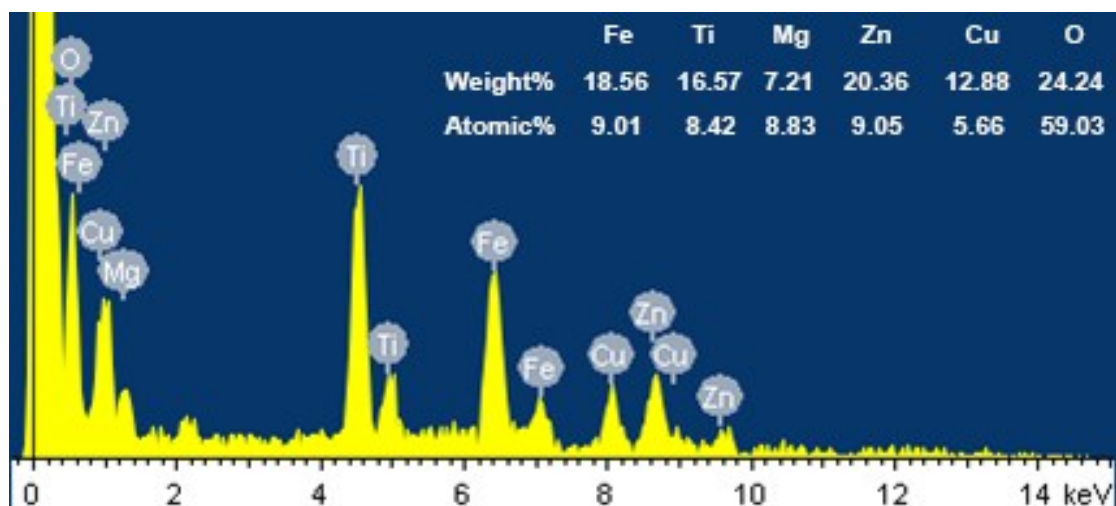


**Fig. S1** EDS analysis result of the synthesized  $(\text{Mg}_{0.2}\text{Ti}_{0.2}\text{Zn}_{0.2}\text{Cu}_{0.2}\text{Fe}_{0.2})_3\text{O}_4$  particles. The corresponding element atomic ratio indicate the homogeneous spatial distributions of each element.

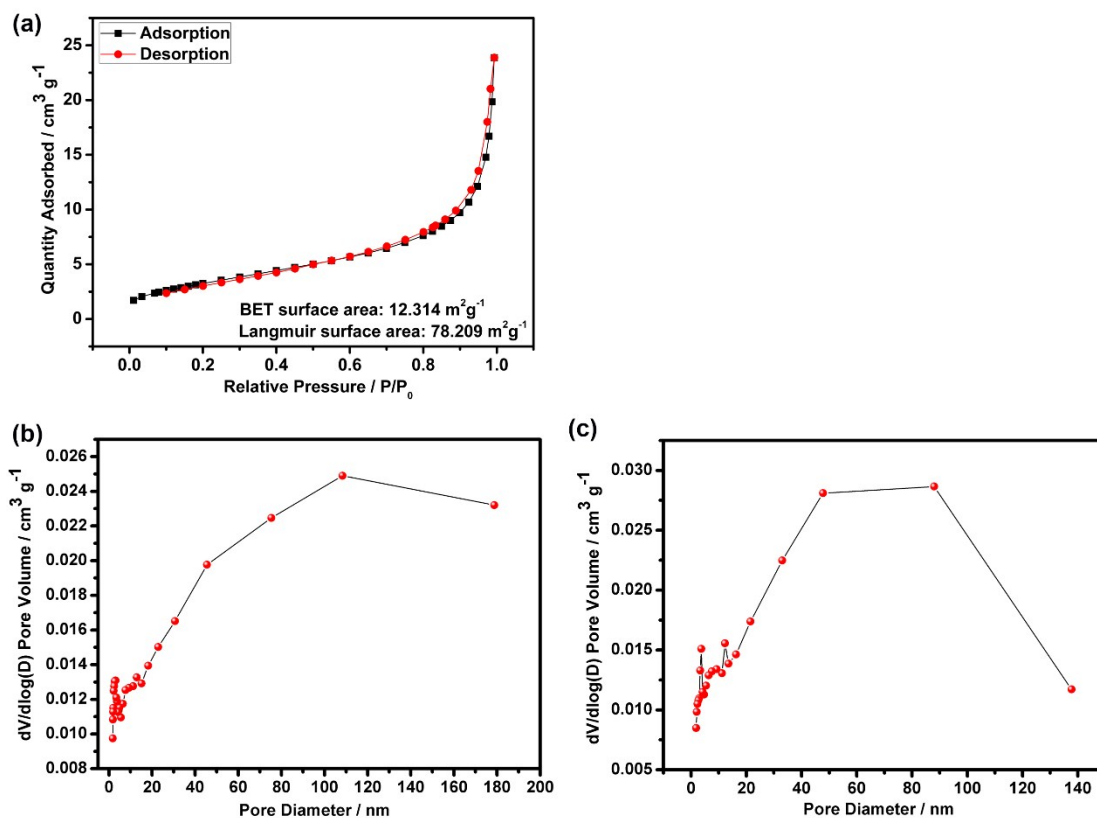


**Fig. S2** (a)  $\text{N}_2$  adsorption-desorption isotherms of the synthesized  $(\text{Mg}_{0.2}\text{Ti}_{0.2}\text{Zn}_{0.2}\text{Cu}_{0.2}\text{Fe}_{0.2})_3\text{O}_4$  particles. The BJH pore size distribution curves based on (b) Adsorption  $dV/d\log(D)$  Pore Volume, (c) Desorption  $dV/d\log(D)$  Pore Volume.

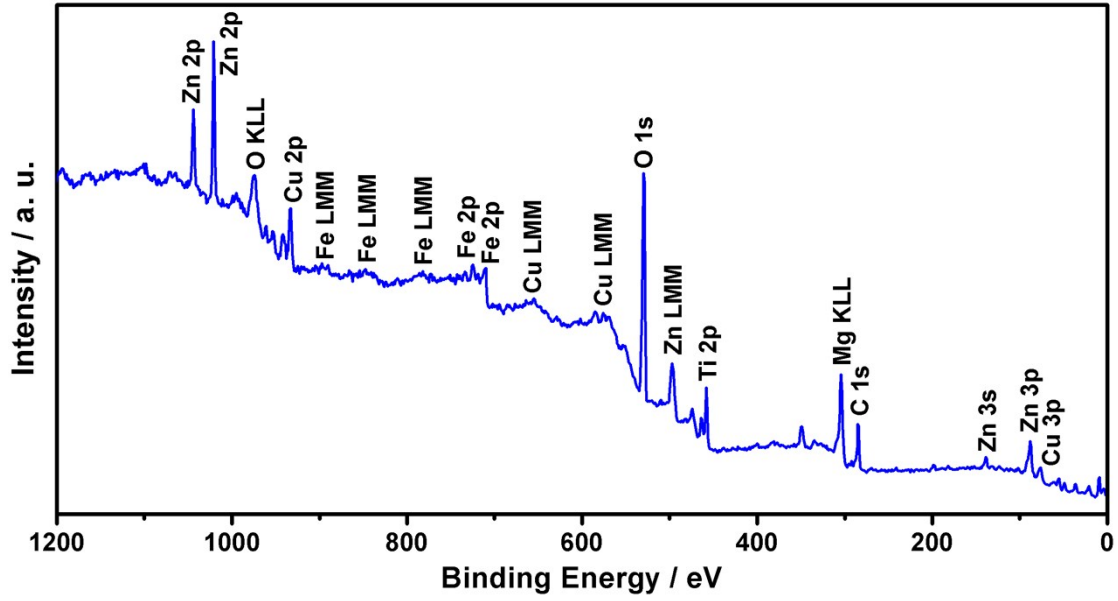


Fig. S3 XPS survey scan spectrum of the synthesized  $(\text{Mg}_{0.2}\text{Ti}_{0.2}\text{Zn}_{0.2}\text{Cu}_{0.2}\text{Fe}_{0.2})_3\text{O}_4$  particles.

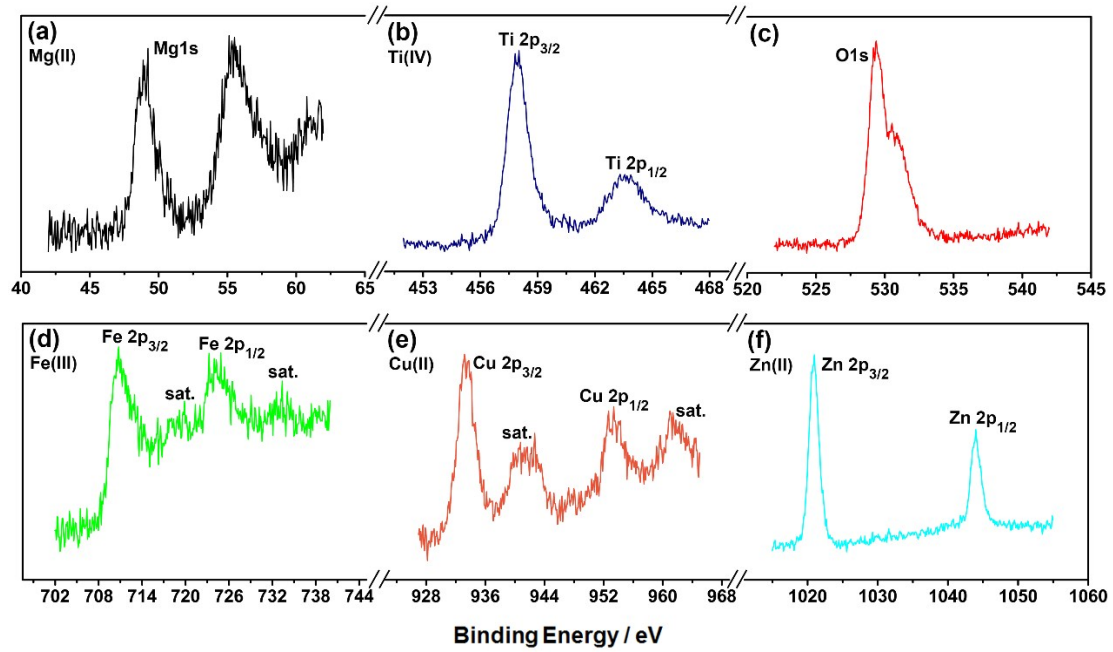
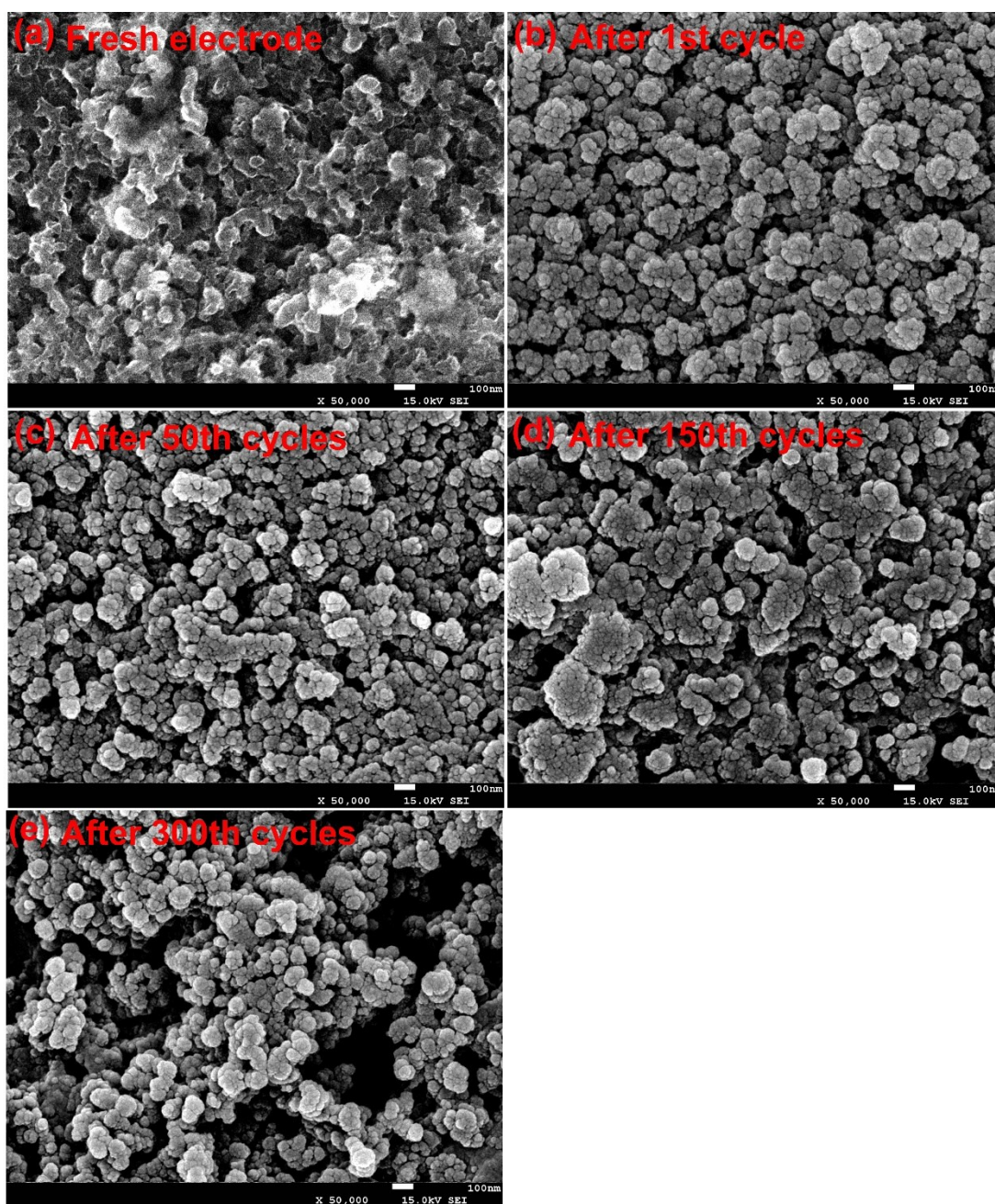
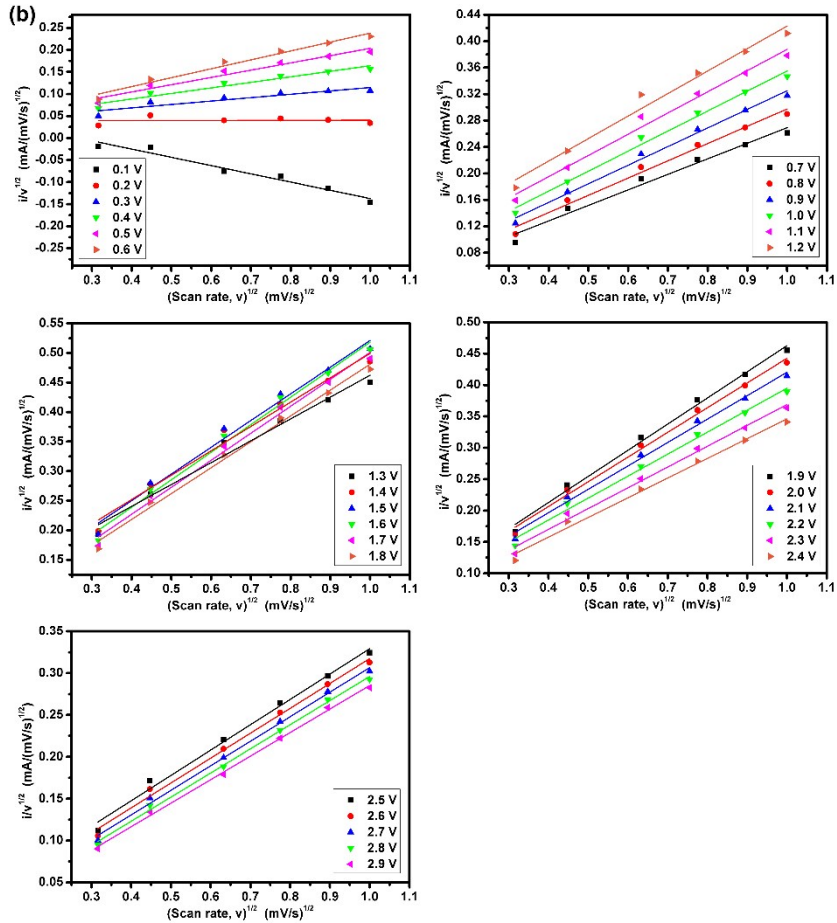
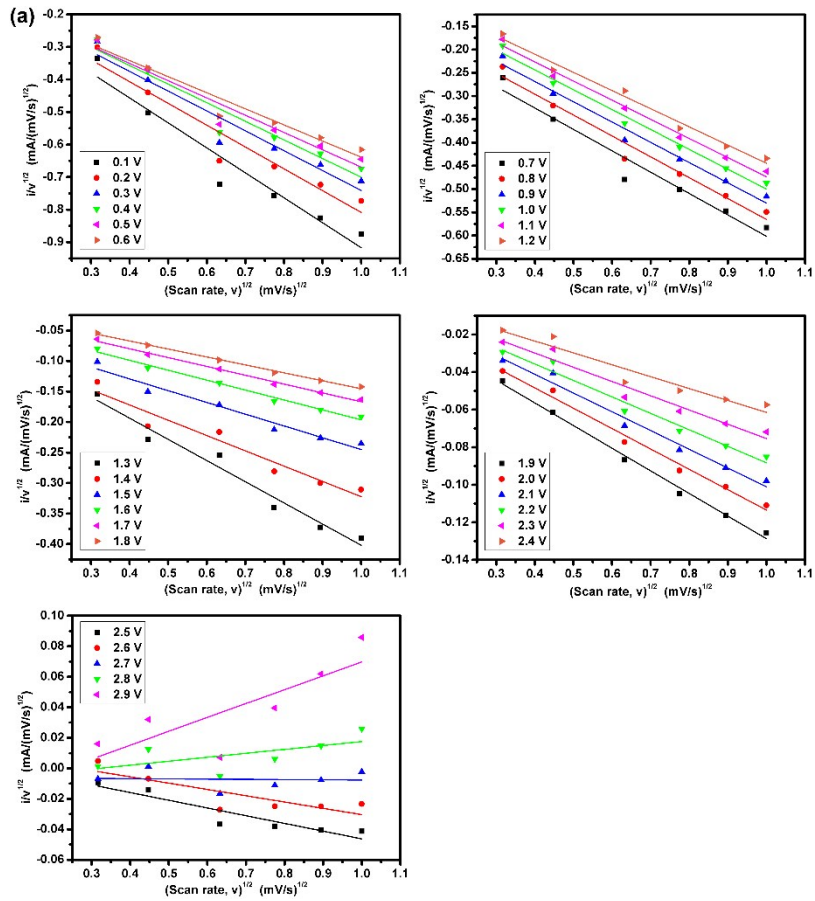


Fig. S4 High-resolution XPS spectra of the synthesized  $(\text{Mg}_{0.2}\text{Ti}_{0.2}\text{Zn}_{0.2}\text{Cu}_{0.2}\text{Fe}_{0.2})_3\text{O}_4$  particles: (a) Mg 1s; (b) Ti 2p; (c) O 1s; (d) Fe 2p; (e) Cu 2p; (f) Zn 2p.



**Fig. S5** SEM results of the evolution process of  $(\text{Mg}_{0.2}\text{Ti}_{0.2}\text{Zn}_{0.2}\text{Cu}_{0.2}\text{Fe}_{0.2})_3\text{O}_4$  electrodes at a current density of  $100 \text{ mA g}^{-1}$ . Surface morphology image of (a) fresh electrode, (b) the electrode at the potential of 3.0 V after 1st discharge/charge cycle, (c) the electrode at the potential of 3.0 V after 50th cycles, (d) the electrode at the potential of 3.0 V after 150th cycles, (e) the electrode at the potential of 3.0 V after 300th cycles.



**Fig. S6** Correlation between the scan rates and corresponding currents of the  $(\text{Mg}_{0.2}\text{Ti}_{0.2}\text{Zn}_{0.2}\text{Cu}_{0.2}\text{Fe}_{0.2})_3\text{O}_4$  electrode at (a) cathodic and (b) anodic scan according to equation:  $i(V)/v^{1/2} = k_1v^{1/2} + k_2$ .

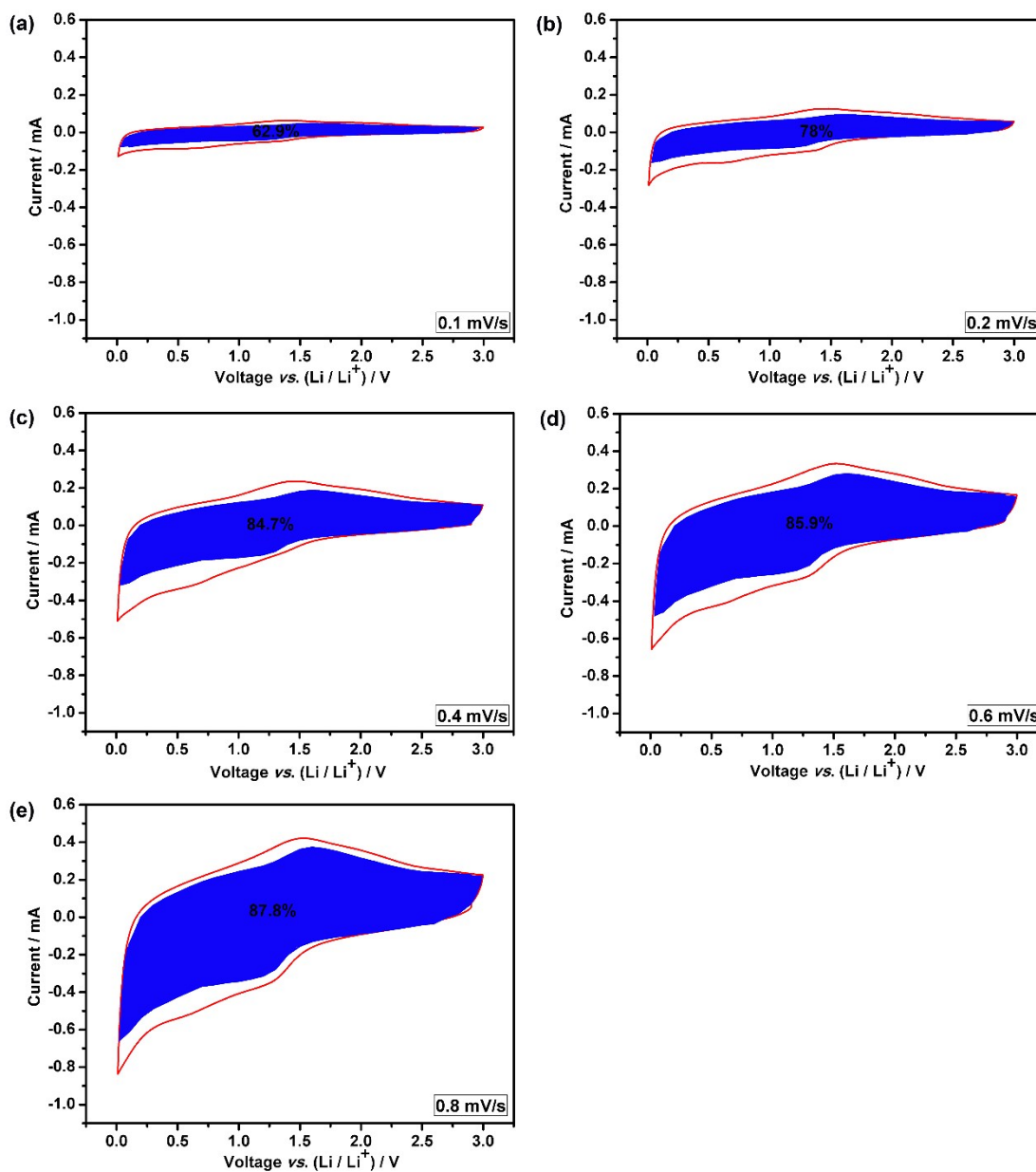


**Fig. S7** The capacitive contribution (blue shaded region) to the total current contribution (red line) for the  $(\text{Mg}_{0.2}\text{Ti}_{0.2}\text{Zn}_{0.2}\text{Cu}_{0.2}\text{Fe}_{0.2})_3\text{O}_4$  electrode at (a) 0.1, (b) 0.2, (c) 0.4, (d) 0.6, (e) 0.8  $\text{mV s}^{-1}$  vs.  $\text{Li}^+/\text{Li}$ .

Compounds	Lattice parameters ( $\text{\AA}$ )	Synthesized temperature ( $^{\circ}\text{C}$ )	BET surface area	References

			(±0.1) m <sup>2</sup> g <sup>-1</sup>	
NiFe <sub>2</sub> O <sub>4</sub>	a = 8.3656(4)	900	6.88	<i>Journal of Physical Chemistry C</i> , <b>2015</b> , 119, 4709-4718.
(Zn <sub>0.25</sub> Ni <sub>0.75</sub> )Fe <sub>2</sub> O <sub>4</sub>	a = 8.3605(6)	900	4.93	<i>Journal of Physical Chemistry C</i> , <b>2015</b> , 119, 4709-4718.
(Zn <sub>0.5</sub> Ni <sub>0.5</sub> )Fe <sub>2</sub> O <sub>4</sub>	a = 8.3590(6)	900	2.25	<i>Journal of Physical Chemistry C</i> , <b>2015</b> , 119, 4709-4718.
(Zn <sub>0.75</sub> Ni <sub>0.25</sub> )Fe <sub>2</sub> O <sub>4</sub>	a = 8.3663(2)	900	4.26	<i>Journal of Physical Chemistry C</i> , <b>2015</b> , 119, 4709-4718.
ZnFe <sub>2</sub> O <sub>4</sub>	a = 8.4375(0)	900	0.79	<i>Journal of Physical Chemistry C</i> , <b>2015</b> , 119, 4709-4718.
5%ZnO.95%Fe <sub>3</sub> O <sub>4</sub>	For ZnO: a = 3.249 c = 5.2046 For Fe <sub>3</sub> O <sub>4</sub> : a = 8.4413	600	10.26	<i>Electrochimica Acta</i> <b>2014</b> , 118, 75-80.
Fe <sub>2</sub> O <sub>3</sub>	a = 5.021 c = 13.734	280	18.95	<i>Electrochimica Acta</i> <b>2014</b> , 118, 75-80.
Fe <sub>2</sub> O <sub>3</sub>	a = 5.041 c = 13.769	900	0.5	<i>Electrochimica Acta</i> <b>2014</b> , 118, 75-80.
(Mg <sub>0.2</sub> Ti <sub>0.2</sub> Zn <sub>0.2</sub> Cu <sub>0.2</sub> Fe <sub>0.2</sub> ) <sub>3</sub> O <sub>4</sub>	a = 8.396	1000	12.31	This Work

**Table S1.** The comparison of lattice parameter, BET surface area values between (Mg<sub>0.2</sub>Ti<sub>0.2</sub>Zn<sub>0.2</sub>Cu<sub>0.2</sub>Fe<sub>0.2</sub>)<sub>3</sub>O<sub>4</sub> and some other solid solutions reported in literature.

Materials	The first	Capacity [mAh]	Capacity	References
-----------	-----------	----------------	----------	------------

	discharge / charge capacities [mAh g <sup>-1</sup> ]	g <sup>-1</sup> / number of cycles	[mAh g <sup>-1</sup> / current density [mA g <sup>-1</sup> ]	
Ni <sub>x</sub> Co <sub>3-x</sub> O <sub>4</sub> nanosheets	2489/1340	1330/50 <sup>th</sup> cycle	293/1600	<i>ACS Applied Materials &amp; Interfaces</i> <b>2014</b> , 6, 9256-9264.
Mesoporous NiCo <sub>2</sub> O <sub>4</sub> microspheres	1712/1214	705/500 <sup>th</sup> cycle	393/1600	<i>ACS Applied Materials &amp; Interfaces</i> <b>2013</b> , 5, 981-988.
Mesoporous ZnCo <sub>2</sub> O <sub>4</sub> microspheres	1600/1205	1256/100 <sup>th</sup> cycle	430/4000	<i>RSC Advances</i> <b>2015</b> , 5, 19241-19247.
Mesoporous ZnCo <sub>2</sub> O <sub>4</sub> microspheres	1332/979	721/80 <sup>th</sup> cycle	382/5000	<i>Journal of Materials Chemistry A</i> <b>2013</b> , 1, 5596-5602.
ZnFe <sub>2</sub> O <sub>4</sub> nanoparticles	1322/933	829/100 <sup>th</sup> cycle	600/1560	<i>RSC Advances</i> <b>2014</b> , 4, 49212-49218.
Hollow CoFe <sub>2</sub> O <sub>4</sub> nanospheres	2264/1230	1185/50 <sup>th</sup> cycle	1030/900	<i>Nanotechnology</i> <b>2012</b> , 23, 055402.
Porous CoFe <sub>2</sub> O <sub>4</sub> nanosheets	1619/1139	806/200 <sup>th</sup> cycle	303/10000	<i>RSC Advances</i> <b>2014</b> , 4, 27488-27492.
Mn <sub>0.5</sub> Co <sub>0.5</sub> Fe <sub>2</sub> O <sub>4</sub> hollow spheres	847/526	498/500 <sup>th</sup> cycle	115/2000	<i>ACS Applied Materials &amp; Interfaces</i> <b>2015</b> , 7, 6300-6309.
Ni <sub>0.33</sub> Mn <sub>0.33</sub> Co <sub>0.33</sub> Fe <sub>2</sub> O <sub>4</sub> mesoporous nanospheres	955/686	490/60 <sup>th</sup> cycle	---	<i>Journal of Materials Chemistry A</i> <b>2014</b> , 2, 5041-5050.
Ni <sub>0.33</sub> Mn <sub>0.33</sub> Co <sub>0.33</sub> Fe <sub>2</sub> O <sub>4</sub> on oxidized carbon nanotubes	1092/692	674/100 <sup>th</sup> cycle	300/1000	<i>RSC Advances</i> <b>2014</b> , 4, 33769-33775.
(Mg <sub>0.2</sub> Ti <sub>0.2</sub> Zn <sub>0.2</sub> Cu <sub>0.2</sub> Fe <sub>0.2</sub> ) <sub>3</sub> O <sub>4</sub>	1261/634	504/300 <sup>th</sup> cycle	268/2000	This work

**Table S2.** Summary of electrochemical performance of different transition metal oxides as anode materials for lithium ion batteries.

Samples	$R_s$ [ $\Omega$ ]	$R_{ct}$ [ $\Omega$ ]	$\sigma$ [ $\Omega$ Hz <sup>1/2</sup> ]	$D_{Li^+}$ [cm <sup>2</sup> s <sup>-1</sup> ]
The fresh half-cell	39.68	283.53	155.52	$1.497 \times 10^{-15}$
The half-cell charged to 3.0 V after 300 cycles	0.07	43.35	87.61	$4.716 \times 10^{-15}$

**Table S3.** The kinetic parameters of the fresh (Mg<sub>0.2</sub>Ti<sub>0.2</sub>Zn<sub>0.2</sub>Cu<sub>0.2</sub>Fe<sub>0.2</sub>)<sub>3</sub>O<sub>4</sub> half-cell (at the open circuit voltage, 3.0 V) and the half-cell charged to 3.0 V after 300 discharge/charge cycles.